Acta Crystallographica Section C
Crystal Structure Communications
ISSN 0108-2701

Conformations and resulting hydrogen-bonded networks of hydrogen {phosphono[(pyridin-1-ium-3-yl)amino]methyl}phosphonate and related 2-chloro and 6-chloro derivatives

Ewa Matczak-Jon[a]* and Katarzyna Ślepokura[b]

[a]Department of Chemistry, Wrocław University of Technology, Wybrzeże Wyspiańskiego 27, 50-370 Wrocław, Poland, and [b]Faculty of Chemistry, University of Wrocław, 14 F. Joliot-Curie Street, 50-383 Wrocław, Poland
Correspondence e-mail: ewa.matczak-jon@pwr.wroc.pl

Received 9 August 2011
Accepted 3 October 2011
Online 15 October 2011

In the crystal structures of the conformational isomers hydrogen {phosphono[(pyridin-1-ium-3-yl)amino]methyl}phosphonate monohydrate (*pro-E*), $C_6H_{10}N_2O_6P_2\cdot H_2O$, (I*a*), and hydrogen {phosphono[(pyridin-1-ium-3-yl)amino]methyl}-phosphonate (*pro-Z*), $C_6H_{10}N_2O_6P_2$, (I*b*), the related hydrogen {[(2-chloropyridin-1-ium-3-yl)amino](phosphono)methyl}-phosphonate (*pro-E*), $C_6H_9ClN_2O_6P_2$, (II), and the salt bis(6-chloropyridin-3-aminium) [hydrogen bis({[2-chloropyridin-1-ium-3-yl(0.5+)]amino}methylenediphosphonate)] (*pro-Z*), $2C_5H_6ClN_2^+\cdot C_{12}H_{16}Cl_2N_4O_{12}P_4^{2-}$, (III), chain–chain interactions involving phosphono ($-PO_3H_2$) and phosphonate ($-PO_3H^-$) groups are dominant in determining the crystal packing. The crystals of (I*a*) and (III) comprise similar ribbons, which are held together by N—H···O interactions, by water- or cation-mediated contacts, and by π–π interactions between the aromatic rings of adjacent zwitterions in (I*a*), and those of the cations and anions in (III). The crystals of (I*b*) and (II) have a layered architecture: the former exhibits highly corrugated monolayers perpendicular to the [100] direction, while in the latter, flat bilayers parallel to the (001) plane are formed. In both (I*b*) and (II), the interlayer contacts are realised through N—H···O hydrogen bonds and weak C—H···O interactions involving aromatic C atoms.

Comment

Pyridine-based bis-phosphonates display a broad spectrum of biological activities which rely predominantly on their inhibitory potency with respect to FPP synthase, a key enzyme in the mevalonate pathway common in human, parasite and plant cells (De Schutter *et al.*, 2010; Sanders *et al.*, 2003; Szabo *et al.*, 2002; Cao *et al.*, 2008). In recent years, we have investigated the crystal structures of a series of [(pyridin-2-yl)-amino]methane-1,1-diphosphonic acids (Matczak-Jon *et al.*, 2001, 2006*a*,*b*, 2009; Matczak-Jon, Ślepokura *et al.*, 2010), which are a subclass of pyridine-based acids with a direct C—N_{amino} bond. Their exceptional feature compared with other members of this family is a partially double C2—N_{amino} bond, which leads to two preferred *Z* and *E* conformers [*Z*/*E* assignment consistent with Matczak-Jon *et al.* (2001)]. During the course of our studies, it has become apparent that the configurational preferences of [(pyridin-2-yl)amino]methane-1,1-diphosphonic acids are primarily determined by the topology and chemical nature of the substituents attached to the pyridine ring. We have demonstrated that compounds substituted in the 4- or 5-position of the pyridine ring exist in solution as a mixture of almost equally populated *Z* and *E* conformers. As long as the pyridine N atom remains protonated, the *Z* conformer crystallizes preferentially (Sanders *et al.*, 2003; Matczak-Jon *et al.*, 2001, 2006*a*,*b*, 2009). The removal of the proton from the pyridinium N atom enables *Z*/*E* interconversion and as a result the *E* form is able to crystallize from solution (Sanders *et al.*, 2003; Matczak-Jon *et al.*, 2009). A key role for the *Z* stabilization, in both the solid state and in solution, is the symmetrical dimer generated through intermolecular bifurcated N—H···O hydrogen bonds involving both exocyclic and pyridine N atoms as proton donors and an O atom of one of the phosphono/phosphonate groups as acceptor. This is a common phenomenon in the crystal structures of all the *Z* zwitterions of [(pyridin-2-yl)amino]methane-1,1-diphosphonic acids studied to date.

In contrast, acids substituted in the 3-position of the pyridine ring adopt the *E* conformation, stabilized through an intramolecular hydrogen bond involving the exocyclic N atom as a proton donor and the sterically accessible substituent as a proton acceptor (Szabo *et al.*, 2002; Matczak-Jon *et al.*, 2001), even in the presence of other substituents attached to the pyridine ring (Matczak-Jon, Ślepokura *et al.*, 2010). This generalization fails only for the zwitterion of [(pyridin-2-yl)-amino]methane-1,1-diphosphonic acid which, despite almost equal populations of the *E* and *Z* conformers in solution, crystallizes as the *E* conformer (Matczak-Jon *et al.*, 2006*a*).

Structural data have not as yet been reported for [(pyridinyl)amino]methane-1,1-diphosphonic acids with the aminomethane-1,1-diphosphonate portion attached to the 3-position of the pyridine ring. These compounds display marked differences in their abilities to bind metal ions in solution (Kowalik-Jankowska *et al.*, 2011) compared with 3-, 4-, 5- and 6-ring-substituted [(pyridin-2-yl)amino]methane-1,1-diphosphonic acids (Matczak-Jon, Kowalik-Jankowska *et al.*, 2010; Matczak-Jon *et al.*, 2002). It is, therefore, highly desirable to look for factors which may be responsible for these differences in their behaviour. We present here the crystal structures of the two conformers of hydrogen {phosphono[(pyridin-1-ium-3-yl)amino]methyl}phosphonate as the monohydrate, (I*a*), and the unsolvated form, (I*b*), the related hydrogen {phosphono[(2-chloropyridin-1-ium-3-yl)amino]-methyl}phosphonate, (II), and the salt bis(6-chloropyridin-3-aminium) [hydrogen bis({[2-chloropyridin-1-ium-3-yl(0.5+)]-

  doi:10.1107/S0108270111040650

amino}methylenediphosphonate)], (III). Principal geometric data are reported in Tables 1, 3, 5 and 7. The asymmetric unit of (I*a*) comprises a zwitterion, formed by proton transfer from one of the phosphono groups to pyridine atom N2, and one water molecule (O1*W* and O2*W*, both located on a twofold axis). Compounds (I*b*) and (II) crystallize as zwitterions with the same protonation scheme as (I*a*). Compound (III) is a salt, in which atoms H2N on N2 and H5 on O5 of the anion both have half-occupancy, and the cation is disordered over two orientations with site occupancies of 0.574 (11) and 0.426 (11) (Figs. 1 and 2, and *Experimental*).

Due to the partial double-bond character of the C3—N1 bond, all four compounds may adopt two different conformations with respect to this bond, labelled *pro-E* and *pro-Z* (IUPAC, 1997). We were successful in obtaining crystals of the *pro-E* and *pro-Z* conformers of (I). On the other hand, the zwitterion of (II) is the *pro-E* conformer, while the bisphosphonate counterpart in (III) adopts the opposite *pro-Z* conformation. This is reflected in the values of the C1—N1—C3—C2 torsion angle of 174.8 (3)° for (I*a*), −3.1 (4)° for (I*b*), 174.8 (2)° for (II) and −17.2 (3)° for (III). In (II), the *pro-E* conformation is additionally stabilized through an intramolecular N1—H1N···Cl1 hydrogen bond. It is also noteworthy that the C3—N1 bonds in (II) and (III) are slightly longer than those found in most of the zwitterions of [(pyridin-2-yl)amino]methane-1,1-diphosphonic acids studied to date (mean value = 1.35 Å; Matczak-Jon *et al.*, 2001, 2006*a*,*b*, 2009; Matczak-Jon, Ślepokura *et al.*, 2010).

As a consequence of the formal sp^2 hybridization of atom N1, atoms N1 and C1 of all compounds are coplanar with the pyridinium ring. However, as seen from the C1—N1—C3—C2 torsion angles (Tables 1, 3, 5 and 7), atom C1 deviates from the pyridinium ring plane more in (III) than in (I*a*), (I*b*) and (II).

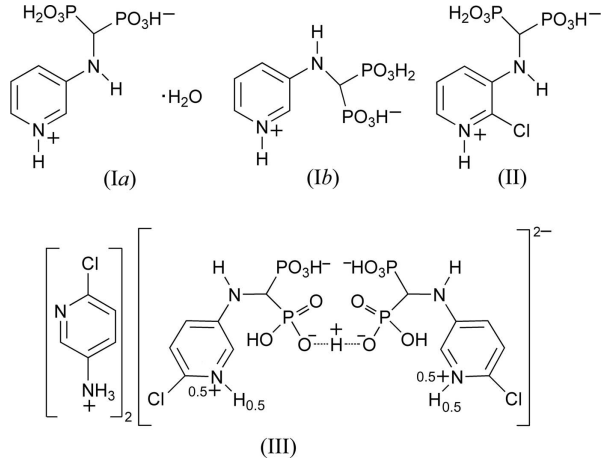

Similar to [(pyridin-2-yl)amino]methane-1,1-diphosphonic acids, a common feature of all four compounds is the planar 'W' conformation of the HO—P—C—P—O sequence, which

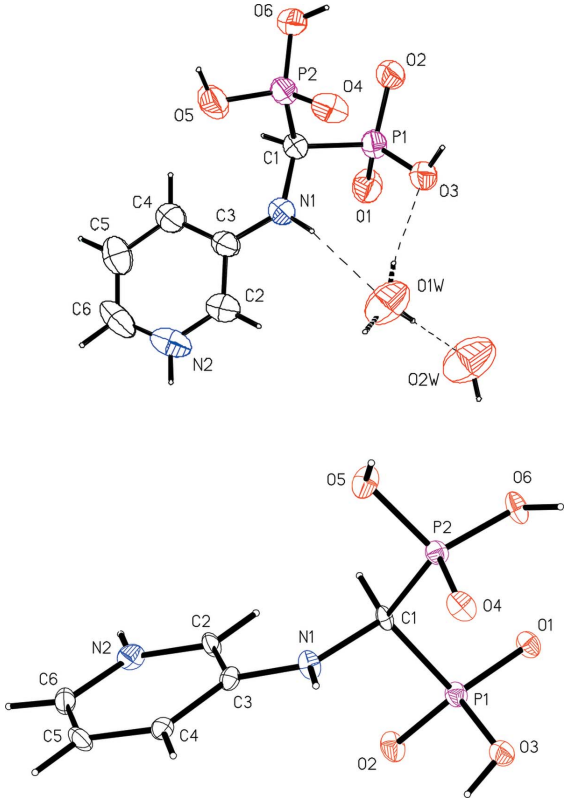

Figure 1
Views of (I*a*) (top) and (I*b*) (bottom), showing the atom-numbering schemes and the symmetry-independent N—H···O and O—H···O hydrogen bonds (thin dashed lines). Displacement ellipsoids are drawn at the 50% probability level. Thick dashed lines indicate covalent bonds to alternative positions of atom H2*W* (related by the action of a twofold axis; site-occupancy factor = 0.5).

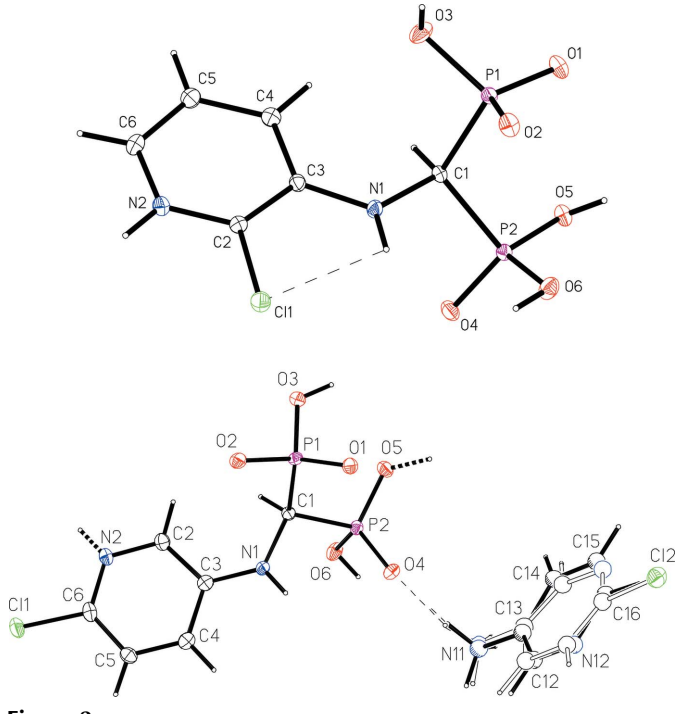

Figure 2
Views of (II) (top) and (III) (bottom), showing the atom-numbering schemes and the intramolecular close contact in (II) and the symmetry-independent intermolecular hydrogen bond in (III) (thin dashed lines). Displacement ellipsoids are drawn at the 50% probability level, except for the C and N atoms of the disordered cation in (III). The two positions of the disordered cation in (III) are shown with solid and open lines. Thick dashed lines indicate covalent bonds to H atoms with a site-occupancy factor of 0.5.

enables the formation of O—H···O hydrogen-bonded chains. As a result, each P atom is antiperiplanar (*ap*) to one of the O atoms from the adjacent phosphonate groups and synclinal (*sc*) to the remaining atoms of this group. In both conformers of (I) and in (II), the O—P—C—P—OH arrangement is nearly planar, which is reflected in the values of the relevant torsion angles: O1/O2—P1—C1—P2 and O5—P2—C1—P1 for (I*a*) and (I*b*), and O3—P1—C1—P2 and O4—P2—C1—P1 for (II) (Tables 1, 3 and 5). The values of the relevant torsion angles for (III), *i.e.* O2—P1—C1—P2 and O6—P2—C1—P1 (Table 7), indicate that atom O6 is the most displaced from the P1—C1—P2 plane compared with the O atoms of (I*a*), (I*b*) and (II).

The orientation of the phosphonate groups relative to the pyridinium ring is defined by the C3—N1—C1—P1 and C3—N1—C1—P2 torsion angles, which reveal that in all four compounds atoms P1 and P2 have an anticlinal orientation with respect to C3.

Consistent with previous observations, the geometry of both the phosphono ($-PO_3H_2$) and phosphonate ($-PO_3H^-$) groups deviates significantly from ideal tetrahedral (Tables 1, 3, 5 and 7). This is mainly reflected in high values of the O1—P1—O2 angle, in which the unprotonated O atoms are involved [average = 115.88 (10)°]. On the other hand, the (H)O—P—C1 angles, in which protonated atoms O3, O5 or O6 are involved, have the smallest value in all four compounds [average = 101.46 (11)°].

In agreement with the crystal structures of [(pyridin-2-yl)-amino]methane-1,1-diphosphonates reported to date, the supramolecular assembly of the zwitterions of (I*a*), (I*b*) and (II) and the monoanions in (III) is determined by chain–chain interactions involving phosphono ($-PO_3H_2$) and phosphonate ($-PO_3H^-$) groups (see Figs. 3 and 4, and Tables 2, 4, 6 and 8).

In (I*a*) and (III), $(-P-C-P-O-H\cdots O)_n$ chains are generated by direct *b*-axis translation through O5—H5···O1^{ii} and O6—H6···O2^{ii} interactions, respectively (symmetry codes in Tables 2 and 8, respectively). As shown in Fig. 3, in both (I*a*) and (III), two bisphosphonate ions from adjacent chains, related to each other by the action of a twofold axis, are joined by other O—H···O hydrogen bonds to form ribbons along the *b* axis. The overall architecture of the ribbons is similar and resembles that observed for related derivatives with 1,3-thiazol-2-yl and 1,3-benzothiazol-2-yl rings (Matczak-Jon, Kowalik-Jankowska *et al.*, 2010). The main difference lies in the number of hydrogen bonds per bisphosphonate pair, which is four in (I*a*) and three in (III). However, while the geometry of both unique chain-linking hydrogen bonds in (I*a*) (O3—H3···O2^{i} and O6—H6···O4^{i}; Table 2) is actually the same, the O3—H3···O1^{i} and O5···H5···O5^{i} hydrogen bonds joining related chains in (III) (Table 8) are of significantly different geometry, resulting from the different strength/energy of the two interactions. Notable is the short *D*···*A* distance [2.403 (3) Å] in the O5···H5···O5^{i} bond, with atom H5 on a twofold axis. Atom H5 was finally refined on a twofold axis at the same distance from the adjacent bisphosphonate anions, which is typical of very strong O—H···O hydrogen bonds, but another model could not be excluded.

Ribbon–ribbon interactions in (I*a*) and (III) are provided mainly by direct hydrogen bonds [N—H···O and C—H···O

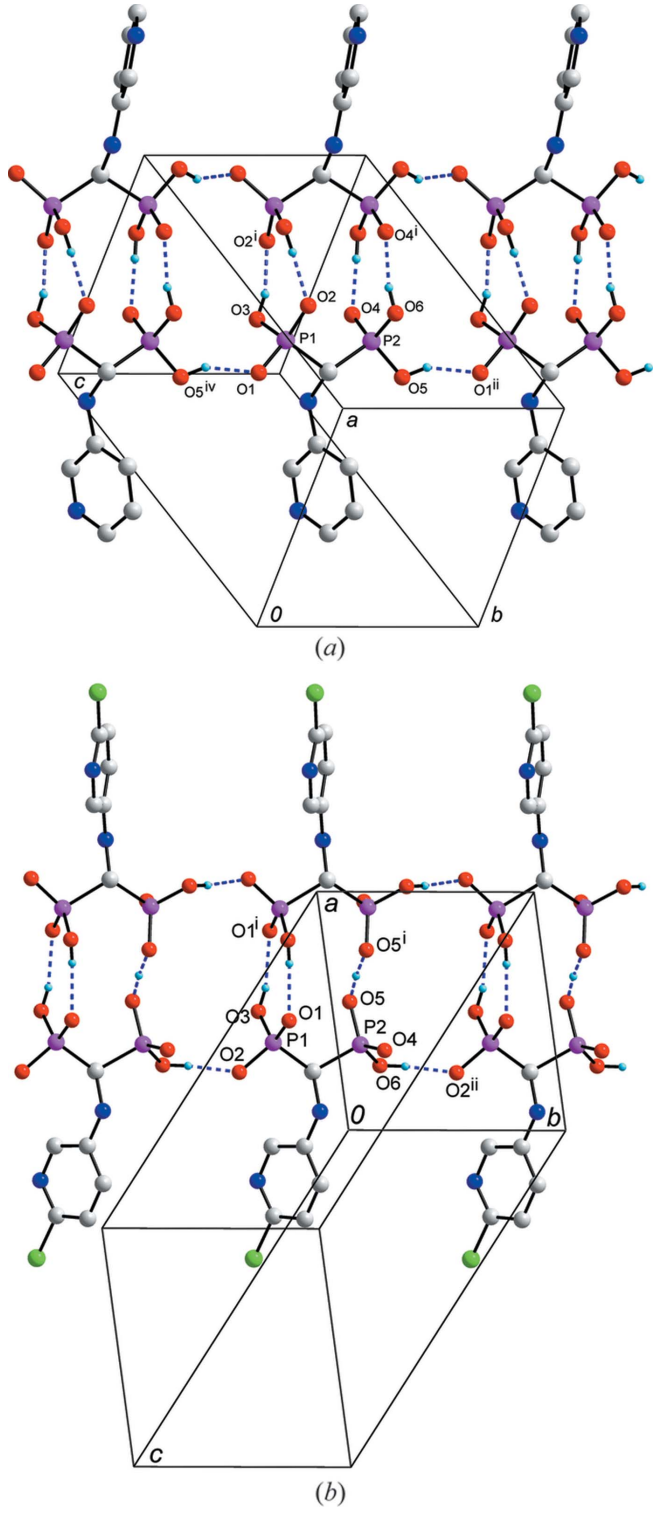

Figure 3
The arrangement of (*a*) the zwitterions in (I*a*) and (*b*) the anions in (III) within the ribbons along the *b* axis. O—H···O hydrogen bonds are shown as dashed lines. H atoms not involved in hydrogen bonding have been omitted for clarity. [Symmetry codes for (I*a*): (i) $-x+\frac{3}{2}, y, -z+\frac{3}{2}$; (ii) $x, y+1, z$; (iv) $x, y-1, z$; symmetry codes for (III): (i) $-x+2, y, -z+\frac{1}{2}$; (ii) $x, y+1, z$.]

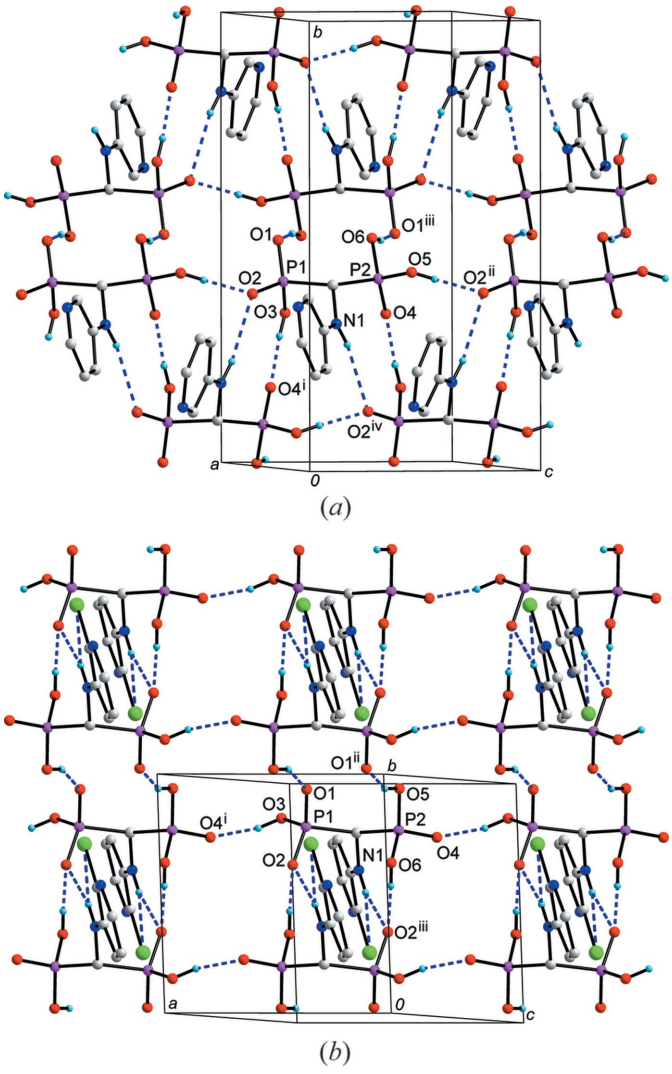

Figure 4
The arrangement of the zwitterions in (*a*) (I*b*) and (*b*) (II) within the layers parallel to the (100) and (001) planes, respectively. O—H···O and N—H···O hydrogen bonds are shown as dashed lines. H atoms not involved in hydrogen bonding have been omitted for clarity. [Symmetry codes for (I*b*): (i) $x, -y+\frac{1}{2}, z-\frac{1}{2}$; (ii) $x, y, z+1$; (iii) $-x+2, -y+1, -z+1$; (iv) $x, -y+\frac{1}{2}, z+\frac{1}{2}$; symmetry codes for (II): (i) $x+1, y, z$; (ii) $-x+1, -y+2, -z+1$; (iii) $-x+1, -y+1, -z+1$.]

in both (I*a*) and (III), and additionally N2—H2N···N2^{iv} and C2—H21···Cl1^{iv} in (III); symmetry code: (iv) $-x+1, -y, -z+1$] and water- or cation-mediated O—H···O [in (I*a*)] or N—H···O and C—H···O [in (III)] contacts. In the crystal structure of (I*a*), water molecules are located on the twofold axis between the ribbons and interact with two zwitterions from two adjacent ribbons each, as well as with each other. Atom O1*W* is in hydrogen-bonding contact with two zwitterions (related by the action of a twofold axis) through N1—H1N···O1*W* and O1*W*—H2*W*···O3 hydrogen bonds, and with the other water molecule *via* O1*W*—H1*W*···O2*W*, as shown in Fig. 1. On the other hand, atom O2*W* interacts with two further zwitterions from the same adjacent ribbon through O2*W*—H3*W*···O4^{iv} and O2*W*—H3*W*···O5^{iv} hydrogen bonds (Table 2). In this way, two hydrogen-bonded water molecules provide inter-ribbon connections by forming hydrogen bonds with four zwitterions from two adjacent ribbons.

An important role is also played by π–π interactions between the aromatic rings of adjacent zwitterions in (I*a*), and of the cations and anions in (III). In (I*a*), the parallel pyridinium rings in the molecules at (x, y, z) and $(-x, -y+1, -z+1)$ have an interplanar spacing of 3.418 (2) Å and a centroid–centroid distance of 3.725 (2) Å. In (III), the pyridinium ring of the anion forms stacking interactions with the cations at $(-x+1, y-1, -z+\frac{1}{2})$ and $(-x+1, y, -z+\frac{1}{2})$, with centroid–centroid separations of 3.80 (1) and 3.90 (1) Å, respectively.

In contrast with (I*a*) and (III), the crystal structures of (I*b*) and (II) have a layered architecture (Fig. 4, and Tables 4 and 6). Here, each $(-P-C-P-O-H\cdots O)_n$ chain, generated by a direct *c*- or *a*-axis translation through O5—H5···O2^{ii} or O3—H3···O4^{i} interactions, respectively (symmetry codes in Tables 4 and 6, respectively), is joined to two adjacent chains of the same type through two significantly different types of interactions. On the one hand, these are centrosymmetric O6—H6···O1^{iii} [in (I*b*), Table 4] and O5—H5···O1^{ii} [in (II), Table 6] hydrogen bonds, resulting in $R_2^2(12)$ and $R_4^4(16)$ rings (Fig. 4) [see Bernstein *et al.* (1995) for hydrogen-bond notation], and this type of interchain connection is the same in (I*b*) and (II). On the other hand, a set of O—H···O and N1—H1N···O hydrogen bonds provides another type of interchain connection which is different in (I*b*) from that in (II) and, therefore, results in different architectures of the layers formed in this way, as shown in Fig. 4. However, the highly corrugated monolayers perpendicular to [100] in (I*b*), and the flat plane bilayers parallel to (001) in (II), have a common feature. This is an arrangement of the individual zwitterions within the layer, locating the aromatic rings at the interlayer exterior. This determines the interactions between adjacent layers. In both (I*b*) and (II), the interlayer contacts are realised mainly through the N2—H2N···O hydrogen bonds and also by weaker C—H···O interactions involving aromatic C atoms (Tables 4 and 6).

In conclusion, chain–chain interactions involving phosphono ($-PO_3H_2$) and phosphonate ($-PO_3H^-$) groups are dominant in determining the crystal packing in all four title compounds. In (I*a*) and (III), O—H···O interactions connect adjacent chains into similar ribbons, which are held together by N—H···O hydrogen bonds [accompanied by N2—H2N···N2^{iv} interactions in (III); symmetry code: (iv) $-x+1, -y, -z+1$], water- or cation-mediated contacts and π–π interactions between aromatic rings. In (I*b*) and (II), the combination of O—H···O and N1—H1N···O intermolecular interactions results in highly corrugated monolayers or flat bilayers, respectively, joined through N2—H2N···O hydrogen bonds and weak C—H···O contacts. In contrast with previously studied [(pyridin-2-yl)amino]methane-1,1-diphosphonic acids, inter- and intramolecular interactions in (I*a*), (I*b*), (II) and (III) can not be expected to provide substantial stabilization of *pro-E* and *pro-Z* conformers in solution. This leads us to speculate that the barrier for *Z*/*E* interconversion in solution for all four compounds is markedly lower than that for aminobisphosphonates with pyridin-2-yl side chains.

Experimental

Compounds (I*a*), (I*b*), (II) and (III) were obtained according to previously described procedures (Sołoducho *et al.*, 1997). Crystals of (I*a*) and (I*b*) were grown in one vessel upon recrystallization from aqueous solution by slow evaporation at room temperature. Crystals of (II) were obtained in a similar way. To obtain crystals of (III), the solid crude product formed upon standing of the reaction mixture was dissolved in water and the solution was allowed to evaporate slowly. The X-ray data for (I*a*) were collected at room temperature (294 K) owing to twinning of the crystal seen in the diffraction pattern at low temperature (100 K).

Spectroscopic analysis for (I) (D_2O, pH = 5.50): ^{1}H NMR (reference TMS, δ, p.p.m.): H1 3.86 ($^3J_{PH}$ = 19.6 Hz), H21 8.00, H41 7.71, H51 7.57, H61 7.81; ^{13}C NMR (reference TMS, δ, p.p.m.): C1 51.16 ($^1J_{PC}$ = 129.9 Hz), C2 124.83, C3 146.80 ($^3J_{PC}$ = 4.2 Hz), C4 127.90, C5 126.76, C6 128.20; ^{31}P NMR (reference 85% H_3PO_4, p.p.m.): δ 14.54.

Spectroscopic analysis for (II) (D_2O, pH = 1.88): ^{1}H NMR (reference TMS, δ, p.p.m.): H1 3.97 ($^3J_{PH}$ = 20.1 Hz), H41 7.40, H51 7.31, H61 7.62; ^{13}C NMR (reference TMS, δ, p.p.m.): C1 50.57 ($^1J_{PC}$ = 133.6 Hz), C2 133.51, C3 141.30 ($^3J_{PC}$ = 4.50 Hz), C4 122.19, C5 124.59, C6 133.76; ^{31}P NMR (reference 85% H_3PO_4, p.p.m.): δ 14.38.

Spectroscopic analysis for (III) (D_2O, pH = 1.92): ^{1}H NMR (reference TMS, δ, p.p.m.): H1 3.90 ($^3J_{PH}$ = 19.7 Hz), H21 7.84, H41 7.36, H51 7.46; ^{13}C NMR (reference TMS, δ, p.p.m.): C1 50.83 ($^1J_{PC}$ = 134.6 Hz), C2 128.87, C3 144.71 ($^3J_{PC}$ = 4.50 Hz), C4 126.31, C5 128.13, C6 132.67; ^{31}P NMR (reference 85% H_3PO_4, p.p.m.): δ 14.61.

Table 1
Selected geometric parameters (Å, °) for (I*a*).

P1—O1	1.507 (2)	P2—O5	1.526 (2)
P1—O2	1.513 (2)	P2—O6	1.536 (2)
P1—O3	1.548 (2)	P2—C1	1.811 (3)
P1—C1	1.820 (3)	N1—C1	1.462 (3)
P2—O4	1.502 (2)	N1—C3	1.360 (4)
O1—P1—O2	115.63 (13)	O5—P2—O6	108.81 (14)
O1—P1—O3	108.77 (12)	O4—P2—C1	108.85 (13)
O2—P1—O3	111.45 (11)	O5—P2—C1	102.22 (14)
O1—P1—C1	105.38 (13)	O6—P2—C1	109.60 (13)
O2—P1—C1	107.42 (12)	C1—N1—C3	125.6 (2)
O3—P1—C1	107.75 (12)	P1—C1—P2	116.41 (14)
O4—P2—O5	113.77 (16)	P1—C1—N1	109.38 (18)
O4—P2—O6	113.01 (12)	P2—C1—N1	109.44 (19)
O1—P1—C1—P2	−170.95 (14)	C3—N1—C1—P2	99.9 (3)
O5—P2—C1—P1	175.87 (17)	C1—N1—C3—C2	174.8 (3)
C3—N1—C1—P1	−131.5 (3)		

Table 2
Hydrogen-bond geometry (Å, °) for (I*a*).

D—H···*A*	*D*—H	H···*A*	*D*···*A*	*D*—H···*A*
O3—H3···O2^{i}	0.82	1.74	2.532 (3)	162
O5—H5···O1^{ii}	0.82	1.67	2.424 (3)	152
O6—H6···O4^{i}	0.82	1.72	2.519 (3)	165
N1—H1N···O1*W*	0.86	2.17	2.938 (4)	148
N2—H2N···O2^{iii}	0.86	2.16	2.911 (4)	146
O1*W*—H1*W*···O2*W*	0.84	1.85	2.689 (6)	180
O1*W*—H2*W*···O3	0.84	2.06	2.859 (2)	160
O2*W*—H3*W*···O4^{iv}	0.84	2.30	3.076 (3)	155
O2*W*—H3*W*···O5^{iv}	0.84	2.55	3.116 (3)	126
C1—H1···O1^{v}	0.98	2.33	3.253 (4)	156
C6—H61···O5^{vi}	0.93	2.48	3.306 (4)	148

Symmetry codes: (i) $-x+\frac{3}{2}, y, -z+\frac{3}{2}$; (ii) $x, y+1, z$; (iii) $x-1, y, z$; (iv) $x, y-1, z$; (v) $-x+1, -y+1, -z+1$; (vi) $-x, -y+2, -z+1$.

Compound (I*a*)

Crystal data

$C_6H_{10}N_2O_6P_2\cdot H_2O$
M_r = 286.12
Monoclinic, $P2/n$
a = 9.068 (3) Å
b = 7.513 (2) Å
c = 16.126 (4) Å
β = 103.55 (3)°
V = 1068.1 (5) Å^3
Z = 4
Mo $K\alpha$ radiation
μ = 0.44 mm^{-1}
T = 294 K
0.38 × 0.30 × 0.15 mm

Data collection

Kuma KM-4-CCD κ-geometry diffractometer with a Sapphire CCD camera
Absorption correction: multi-scan (*CrysAlis RED*; Oxford Diffraction, 2009)
T_{min} = 0.880, T_{max} = 1.000
9984 measured reflections
2907 independent reflections
2229 reflections with $I > 2\sigma(I)$
R_{int} = 0.034

Refinement

$R[F^2 > 2\sigma(F^2)]$ = 0.055
$wR(F^2)$ = 0.134
S = 1.06
2907 reflections
164 parameters
4 restraints
H atoms treated by a mixture of independent and constrained refinement
$\Delta\rho_{max}$ = 0.52 e Å^{-3}
$\Delta\rho_{min}$ = −0.27 e Å^{-3}

Compound (I*b*)

Crystal data

$C_6H_{10}N_2O_6P_2$
M_r = 268.10
Monoclinic, $P2_1/c$
a = 9.172 (3) Å
b = 14.802 (4) Å
c = 7.589 (2) Å
β = 104.35 (3)°
V = 998.2 (5) Å^3
Z = 4
Mo $K\alpha$ radiation
μ = 0.45 mm^{-1}
T = 120 K
0.20 × 0.02 × 0.01 mm

Data collection

Oxford Xcalibur PX κ-geometry diffractometer with an Onyx CCD camera
Absorption correction: analytical (*CrysAlis RED*; Oxford Diffraction, 2009)
T_{min} = 0.954, T_{max} = 0.994
17046 measured reflections
2925 independent reflections
1307 reflections with $I > 2\sigma(I)$
R_{int} = 0.168

Refinement

$R[F^2 > 2\sigma(F^2)]$ = 0.048
$wR(F^2)$ = 0.056
S = 0.82
2925 reflections
148 parameters
H-atom parameters constrained
$\Delta\rho_{max}$ = 0.46 e Å^{-3}
$\Delta\rho_{min}$ = −0.51 e Å^{-3}

Compound (II)

Crystal data

$C_6H_9ClN_2O_6P_2$
M_r = 302.54
Triclinic, $P\overline{1}$
a = 7.667 (2) Å
b = 8.364 (2) Å
c = 9.283 (3) Å
α = 109.41 (3)°
β = 105.31 (3)°
γ = 92.39 (3)°
V = 536.0 (3) Å^3
Z = 2
Mo $K\alpha$ radiation
μ = 0.67 mm^{-1}
T = 100 K
0.47 × 0.18 × 0.06 mm

Table 3
Selected geometric parameters (Å, °) for (I*b*).

P1—O1	1.504 (2)	P2—O5	1.5405 (19)
P1—O2	1.5100 (18)	P2—O6	1.544 (2)
P1—O3	1.556 (2)	P2—C1	1.825 (2)
P1—C1	1.834 (2)	N1—C1	1.460 (3)
P2—O4	1.4812 (19)	N1—C3	1.366 (3)
O1—P1—O2	116.63 (10)	O5—P2—O6	108.31 (12)
O1—P1—O3	107.19 (12)	O4—P2—C1	112.75 (12)
O2—P1—O3	111.83 (11)	O5—P2—C1	101.85 (11)
O1—P1—C1	110.27 (12)	O6—P2—C1	104.73 (11)
O2—P1—C1	104.72 (11)	C1—N1—C3	124.4 (2)
O3—P1—C1	105.70 (12)	P1—C1—P2	117.34 (14)
O4—P2—O5	114.35 (11)	P1—C1—N1	110.51 (17)
O4—P2—O6	113.78 (12)	P2—C1—N1	107.66 (16)
O2—P1—C1—P2	172.42 (14)	C3—N1—C1—P2	141.8 (2)
O5—P2—C1—P1	165.67 (15)	C1—N1—C3—C2	−3.1 (4)
C3—N1—C1—P1	−88.9 (3)		

Table 4
Hydrogen-bond geometry (Å, °) for (I*b*).

D—H···*A*	*D*—H	H···*A*	*D*···*A*	*D*—H···*A*
O3—H3···O4^{i}	0.84	1.71	2.514 (2)	159
O5—H5···O2^{ii}	0.84	1.67	2.479 (2)	161
O6—H6···O1^{iii}	0.84	1.76	2.586 (3)	167
N1—H1N···O2^{iv}	0.88	2.35	3.193 (3)	160
N2—H2N···O1^{v}	0.88	1.90	2.733 (3)	157
C2—H21···O5^{vi}	0.95	2.58	3.220 (3)	125
C4—H41···O2^{iv}	0.95	2.59	3.402 (3)	144
C6—H61···O3^{vii}	0.95	2.45	3.196 (3)	136
C6—H61···O4^{viii}	0.95	2.55	3.346 (4)	142

Symmetry codes: (i) $x, -y+\frac{1}{2}, z-\frac{1}{2}$; (ii) $x, y, z+1$; (iii) $-x+2, -y+1, -z+1$; (iv) $x, -y+\frac{1}{2}, z+\frac{1}{2}$; (v) $-x+1, -y+1, -z$; (vi) $-x+1, -y+1, -z+1$; (vii) $x-1, -y+\frac{1}{2}, z-\frac{1}{2}$; (viii) $x-1, y, z-1$.

Table 5
Selected geometric parameters (Å, °) for (II).

P1—O1	1.5018 (11)	P2—O5	1.5217 (11)
P1—O2	1.5092 (13)	P2—O6	1.5434 (14)
P1—O3	1.5617 (13)	P2—C1	1.8288 (16)
P1—C1	1.8315 (15)	N1—C1	1.4634 (17)
P2—O4	1.5124 (12)	N1—C3	1.3671 (18)
O1—P1—O2	115.63 (7)	O5—P2—O6	109.96 (7)
O1—P1—O3	110.53 (7)	O4—P2—C1	106.49 (7)
O2—P1—O3	112.38 (7)	O5—P2—C1	108.88 (7)
O1—P1—C1	107.64 (7)	O6—P2—C1	107.06 (7)
O2—P1—C1	110.20 (7)	C1—N1—C3	123.75 (12)
O3—P1—C1	99.10 (7)	P1—C1—P2	115.93 (7)
O4—P2—O5	110.88 (7)	P1—C1—N1	110.38 (10)
O4—P2—O6	113.35 (7)	P2—C1—N1	109.95 (10)
O3—P1—C1—P2	164.71 (8)	C3—N1—C1—P2	−139.37 (13)
O4—P2—C1—P1	178.28 (7)	C1—N1—C3—C2	174.83 (13)
C3—N1—C1—P1	91.50 (15)		

Data collection

Kuma KM-4-CCD κ-geometry diffractometer with a Sapphire CCD camera
Absorption correction: multi-scan (*CrysAlis RED*; Oxford Diffraction, 2009)
T_{min} = 0.920, T_{max} = 1.000
6017 measured reflections
2735 independent reflections
2503 reflections with $I > 2\sigma(I)$
R_{int} = 0.016

Table 6
Hydrogen-bond geometry (Å, °) for (II).

D—H···*A*	*D*—H	H···*A*	*D*···*A*	*D*—H···*A*
O3—H3···O4^{i}	0.84	1.80	2.540 (2)	146
O5—H5···O1^{ii}	0.84	1.64	2.424 (2)	153
O6—H6···O2^{iii}	0.84	1.63	2.461 (2)	173
N1—H1N···Cl1	0.88	2.57	3.002 (2)	111
N1—H1N···O2^{iii}	0.88	2.27	3.103 (2)	158
N2—H2N···O4^{iv}	0.88	1.81	2.649 (2)	159
C4—H41···O3	0.95	2.52	3.042 (2)	115
C5—H51···O1^{v}	0.95	2.54	3.429 (3)	156
C6—H61···O6^{vi}	0.95	2.32	3.131 (2)	143

Symmetry codes: (i) $x+1, y, z$; (ii) $-x+1, -y+2, -z+1$; (iii) $-x+1, -y+1, -z+1$; (iv) $-x+1, -y+1, -z+2$; (v) $-x+2, -y+2, -z+2$; (vi) $x+1, y, z+1$.

Refinement

$R[F^2 > 2\sigma(F^2)]$ = 0.027
$wR(F^2)$ = 0.075
S = 1.06
2735 reflections
157 parameters
H-atom parameters constrained
$\Delta\rho_{max}$ = 0.44 e Å^{-3}
$\Delta\rho_{min}$ = −0.64 e Å^{-3}

Compound (III)

Crystal data

$2C_5H_6ClN_2^+\cdot C_{12}H_{16}Cl_2N_4O_{12}P_4^{2-}$
M_r = 862.20
Monoclinic, $P2/c$
a = 8.555 (2) Å
b = 7.585 (2) Å
c = 24.560 (5) Å
β = 94.32 (3)°
V = 1589.2 (6) Å^3
Z = 2
Mo $K\alpha$ radiation
μ = 0.65 mm^{-1}
T = 100 K
0.25 × 0.11 × 0.03 mm

Data collection

Kuma KM-4-CCD κ-geometry diffractometer with a Sapphire CCD camera
Absorption correction: analytical (*CrysAlis RED*; Oxford Diffraction, 2009)
T_{min} = 0.895, T_{max} = 0.976
16241 measured reflections
4513 independent reflections
3162 reflections with $I > 2\sigma(I)$
R_{int} = 0.056

Table 7
Selected geometric parameters (Å, °) for (III).

P1—O1	1.5070 (16)	P2—O5	1.5164 (16)
P1—O2	1.5112 (15)	P2—O6	1.5644 (15)
P1—O3	1.5754 (16)	P2—C1	1.815 (2)
P1—C1	1.835 (2)	N1—C1	1.458 (3)
P2—O4	1.5016 (16)	N1—C3	1.367 (3)
O1—P1—O2	115.64 (9)	O5—P2—O6	108.01 (9)
O1—P1—O3	110.31 (9)	O4—P2—C1	108.95 (9)
O2—P1—O3	107.95 (8)	O5—P2—C1	106.37 (9)
O1—P1—C1	112.76 (9)	O6—P2—C1	102.69 (9)
O2—P1—C1	105.56 (9)	C1—N1—C3	123.81 (18)
O3—P1—C1	103.82 (9)	P1—C1—P2	113.86 (11)
O4—P2—O5	116.75 (9)	P1—C1—N1	114.15 (14)
O4—P2—O6	112.96 (9)	P2—C1—N1	109.54 (13)
O2—P1—C1—P2	−170.13 (10)	C3—N1—C1—P2	−131.28 (17)
O6—P2—C1—P1	−155.56 (11)	C1—N1—C3—C2	−17.2 (3)
C3—N1—C1—P1	99.7 (2)		

Table 8
Hydrogen-bond geometry (Å, °) for (III).

D—H···A	D—H	H···A	D···A	D—H···A
O3—H3···O1^{i}	0.84	1.91	2.729 (2)	164
O5—H5···O5^{i}	1.20 (1)	1.20 (1)	2.403 (3)	173 (5)
O6—H6···O2^{ii}	0.84	1.71	2.543 (2)	171
N1—H1N···O4^{iii}	0.88	2.35	3.115 (2)	145
N2—H2N···N2^{iv}	0.88	1.91	2.791 (4)	179
N11—H11*A*···O1^{ii}	0.91	1.89	2.778 (12)	166
N11—H11*B*···O4	0.91	1.80	2.697 (11)	169
N11—H11*C*···O2^{v}	0.91	1.86	2.763 (11)	172
N110—H11*D*···O1^{ii}	0.91	1.84	2.742 (15)	168
N110—H11*E*···O4	0.91	1.76	2.651 (16)	165
N110—H11*F*···O2^{v}	0.91	1.95	2.850 (14)	172
C2—H21···Cl1^{iv}	0.95	2.78	3.506 (2)	134
C4—H41···O4^{iii}	0.95	2.59	3.379 (3)	140
C12—H12···O6^{iii}	0.95	2.49	3.337 (7)	148
C14—H14···O3^{vi}	0.95	2.51	3.180 (6)	128
C120—H120···O3^{vi}	0.95	2.37	3.189 (8)	144
C140—H140···O6^{iii}	0.95	2.28	3.174 (7)	156
C150—H150···N12^{vii}	0.95	2.49	3.365 (6)	153

Symmetry codes: (i) $-x+2, y, -z+\frac{1}{2}$; (ii) $x, y+1, z$; (iii) $-x+1, y, -z+\frac{1}{2}$; (iv) $-x+1, -y, -z+1$; (v) $-x+1, y+1, -z+\frac{1}{2}$; (vi) $-x+2, y+1, -z+\frac{1}{2}$; (vii) $-x+1, -y+1, -z$.

Refinement

$R[F^2 > 2\sigma(F^2)] = 0.041$
$wR(F^2) = 0.090$
$S = 1.02$
4513 reflections
226 parameters
18 restraints
H atoms treated by a mixture of independent and constrained refinement
$\Delta\rho_{max} = 0.46$ e Å^{-3}
$\Delta\rho_{min} = -0.59$ e Å^{-3}

The 6-chloropyridin-3-aminium cation in (III) is disordered over two positions [site-occupation factors = 0.574 (11) and 0.426 (11)], corresponding to its two different orientations (Fig. 2). In the final model, the equivalent bond lengths and angles of the two positions were restrained to be similar using the SAME instruction (*SHELXL97*; Sheldrick, 2008). The positions of the Cl atoms (Cl2 and Cl20) were refined with the same fractional coordinates and anisotropic displacement parameters (constraints were applied with the EXYZ and EADP instructions in *SHELXL97*).

Non-H atoms were refined anisotropically, except for the C and N atoms of both positions of the disordered 6-chloropyridin-3-aminium cation in (III). All H atoms were found in difference Fourier maps. Atom H5 in (III) is located on a twofold axis between two anions, 1.20 (1) Å from each O5 atom, and was refined isotropically. Atom H2*W* bound to O1*W* in (I*a*) was refined with a site-occupation factor of 0.5, which results in two alternative positions for this atom, related by the action of a twofold axis (Fig. 1). In the final refinement cycles, all water H atoms in (I*a*) were refined with O—H and H···H distances restrained to 0.84 (6) and 1.36 (6) Å, respectively, and with U_{iso}(H) = 1.5U_{eq}(O). All remaining H atoms were treated as riding atoms in geometrically optimized positions, with C—H = 0.93–1.00 Å, N—H = 0.86–0.91 Å and O—H = 0.82–0.84 Å, and with U_{iso}(H) = 1.2U_{eq}(C,N) for CH and NH, or 1.5U_{eq}(N,O) for NH_3 and OH. Atom H2N in (III) was refined with a site-occupation factor of 0.5 due to a hydrogen bond formed between adjacent molecules, in which atom N2 is both donor and acceptor, *viz.* N—H2N···N2^{iv}. For (I*b*), a weighting parameter of $a = 0$ was used to get a more reasonable goodness-of-fit value.

For all four compounds, data collection: *CrysAlis CCD* (Oxford Diffraction, 2009); cell refinement: *CrysAlis RED* (Oxford Diffraction, 2009); data reduction: *CrysAlis RED*; program(s) used to solve structure: *SHELXS97* (Sheldrick, 2008); program(s) used to refine structure: *SHELXL97* (Sheldrick, 2008); molecular graphics: *XP* (Bruker, 1998) and *DIAMOND* (Brandenburg, 2005); software used to prepare material for publication: *SHELXL97*.

The authors express their gratitude to Professor Paweł Kafarski for supplying the samples of the studied compounds. Financial support from the Chemistry Department, Wrocław University of Technology, is gratefully acknowledged.

Supplementary data for this paper are available from the IUCr electronic archives (Reference: FG3227). Services for accessing these data are described at the back of the journal.

References

Bernstein, J., Davis, R. E., Shimoni, L. & Chang, N.-L. (1995). *Angew. Chem. Int. Ed. Engl.* **34**, 1555–1573.
Brandenburg, K. (2005). *DIAMOND*. Version 3.0. Crystal Impact GbR, Bonn, Germany.
Bruker (1998). *XP*. Version 5.1. Bruker AXS Inc., Madison, Wisconsin, USA.
Cao, R., Chen, C. K.-M., Guo, R.-T., Wang, A. H.-J. & Oldfield, E. (2008). *Proteins*, **73**, 431–439.
De Schutter, J. W., Zaretsky, S., Welbourn, S., Pause, A. & Tsantrizos, Y. S. (2010). *Bioorg. Med. Chem. Lett.* **20**, 5781–5786.
IUPAC (1997). *IUPAC Compendium of Chemical Terminology* (the 'Gold Book'), compiled by A. D. McNaught & A. Wilkinson, 2nd ed. Oxford: Blackwell Scientific Publications.
Kowalik-Jankowska, T., Pietruszka, M., Jezierska, J., Matczak-Jon, E. & Kafarski, P. (2011). *Polyhedron*, **30**, 1274–1280.
Matczak-Jon, E., Kowalik-Jankowska, T., Ślepokura, K., Kafarski, P. & Rajewska, A. (2010). *Dalton Trans.* **39**, 1207–1221.
Matczak-Jon, E., Kurzak, B., Kamecka, A. & Kafarski, P. (2002). *Polyhedron*, **21**, 321–332.
Matczak-Jon, E., Sawka-Dobrowolska, W., Kafarski, P. & Videnova-Adrabińska, V. (2001). *New J. Chem.* **25**, 1447–1457.
Matczak-Jon, E., Ślepokura, K. & Kafarski, P. (2006*a*). *J. Mol. Struct.* **782**, 81–93.
Matczak-Jon, E., Ślepokura, K. & Kafarski, P. (2006*b*). *Acta Cryst.* C**62**, o132–o135.
Matczak-Jon, E., Ślepokura, K., Kafarski, P., Skrzyńska, I. & Jon, M. (2009). *Acta Cryst.* C**65**, o261–o266.
Matczak-Jon, E., Ślepokura, K., Zierkiewicz, W., Kafarski, P. & Dąbrowska, E. (2010). *J. Mol. Struct.* **980**, 182–192.
Oxford Diffraction (2009). *CrysAlis CCD* and *CrysAlis RED*. In Xcalibur PX and Kuma KM-4-CCD software. Versions 1.171.33.42. Oxford Diffraction Ltd, Yarnton, Oxfordshire, England.
Sanders, J. M., Gomez, A. O., Mao, J., Meints, G. A., Van Brusel, E. M., Burzyńska, A., Kafarski, P., Gonzalez-Pacanowska, D. & Oldfield, E. (2003). *J. Med. Chem.* **46**, 5171–5183.
Sheldrick, G. M. (2008). *Acta Cryst.* A**64**, 112–122.
Sołoducho, J., Gancarz, R., Wieczorek, P., Korf, J., Hafnem, J., Lejczak, B. & Kafarski, P. (1997). Patent PL 172268B1.
Szabo, C. M., Martin, M. B. & Oldfield, E. (2002). *J. Med. Chem.* **45**, 2894–2903.